PAPER

Wireless-Powered Filter-and-Forward Relaying in Frequency-Selective Channels

Junta FURUKAWA[†*], ***Student Member***, **Teruyuki MIYAJIMA**[†a)], ***and*** **Yoshiki SUGITANI**[†b)], ***Members***

SUMMARY In this paper, we propose a filter-and-forward relay scheme with energy harvesting for single-carrier transmission in frequency-selective channels. The relay node harvests energy from both the source node transmit signal and its own transmit signal by self-energy recycling. The signal received by the relay node is filtered to suppress the inter-symbol interference and then forwarded to the destination node using the harvested energy. We consider a filter design method based on the signal-to-interference-plus-noise power ratio maximization, subject to a constraint that limits the relay transmit power. In addition, we provide a golden-section search based algorithm to optimize the power splitting ratio of the power splitting protocol. The simulation results show that filtering and self-energy recycling of the proposed scheme are effective in improving performance. It is also shown that the proposed scheme is useful even when only partial channel state information is available.

key words: *wireless energy harvesting, filter-and-forward relaying, inter-symbol interference, self-energy recycling, full-duplex*

1. Introduction

Wireless energy harvesting (WEH) is considered as a promising technology to prolong the lifetime of energy constrained wireless nodes [1], [2]. Especially, simultaneous wireless information and power transfer (SWIPT) technology using radio frequency (RF) signals has attracted significant attention to wireless communications, such as the Internet of Things (IoT) and 5G networks [3]. A potential application of SWIPT is relay networks, where a relay node with a nominal battery capacity can harvest energy from the RF signal that is conveying information from a source node [3]. This makes relay nodes independent of battery exchange or recharging, which is expensive and inconvenient [4].

Several studies on relay transmissions using WEH have been conducted till date [3], [5]. In the pioneering study [5], Nasir et al. considered an amplify-and-forward (AF) relay scheme with WEH, in which a relay node simply forwards a properly scaled signal using the energy harvested from the signal transmitted by the source node. Although the AF scheme successfully operates in frequency-flat channels, it suffers from performance degradation in wideband communications over frequency-selective channels, due to inter-symbol interference (ISI). A common approach to combat ISI in AF relaying is to apply orthogonal frequency division multiplexing (OFDM) with cyclic prefix (CP). However, OFDM is not suitable for EH-based relay nodes that have limited power supply. This is because the power amplifier efficiency of OFDM is significantly low due to a high peak-to-average power ratio, and the bandwidth efficiency is reduced due to the existence of CP. In addition, OFDM is sensitive to hardware impairments, such as phase noise and transceiver I/Q imbalance, in low power devices. Meanwhile, an alternative approach to suppress ISI is to employ a filter-and-forward (FF) relay scheme [6], where a relay node processes received signals by a time-domain FIR filter and forwards the output. Since the FF scheme can be applied to single-carrier transmission without CP, the above-mentioned drawbacks of OFDM can be avoided. So far, there has been no report on the development of an FF relay scheme using WEH.

More recently, a new EH technique called self-energy recycling has been studied in [7]–[10]. In the self-energy recycling systems, EH nodes operate in full-duplex mode and harvest energy from their own transmitted RF signal. Then, the so-called self-interference signal at full-duplex nodes turns to be beneficial as it provides additional energy. In [7]–[10], the authors considered AF relay schemes with self-energy recycling, where a relay node operating in full-duplex mode harvests energy from the received signal and forwards the amplified signal using the harvested energy simultaneously. It has been reported in [7] that the AF scheme with self-energy recycling is superior to the time switching protocol based AF scheme without self-energy recycling, in frequency-flat channels. To the best of our knowledge, self-energy recycling has not yet been applied to FF relaying in frequency-selective channels.

In this paper, we propose a FF relay scheme with self-energy recycling for single-carrier transmissions without CP. In the proposed scheme, the relay node effectively suppresses ISI in frequency-selective channels by using FIR filters, and is energy efficient owing to self-energy recycling and EH from the signal transmitted by the source node. The filter coefficients are designed to maximize signal-to-interference-plus-noise power ratio (SINR) at the destination node, with a constraint to limit relay transmission power. As the proposed scheme is based on the power splitting (PS) protocol, the power splitting ratio is optimized using the golden-section search. In addition, a filter design for a partial channel state information (CSI) case is considered, where only second-order statistics of relay-to-destination channels are available.

Throughout this paper, the following notations are used:

Manuscript received October 25, 2019.
Manuscript revised March 18, 2020.
[†]The authors are with the Graduate School of Science and Engineering, Ibaraki University, Hitachi-shi, 316-8511 Japan.
[*]Presently, with NTT Electronics Corp.
a) E-mail: teruyuki.miyajima.spc@vc.ibaraki.ac.jp
b) E-mail: yoshiki.sugitani.0301@vc.ibaraki.ac.jp
DOI: 10.1587/transfun.2019EAP1150

$(\cdot)^T$, $(\cdot)^H$, and $(\cdot)^*$ indicate the transpose, Hermitian transpose, and complex conjugate of a vector or matrix, respectively. $\otimes$ denotes the Kronecker product, $*$ denotes convolution, $\mathbf{0}_{N\times M}$ is a $N \times M$ matrix whose elements are all zero, $\mathbf{I}_N$ denotes the $N \times N$ identity matrix, $\mathbf{e}_m$ is the mth column of the identity matrix, toeplitz$(\mathbf{A}_{N\times M}, L)$ refers to a $NL \times (M + L - 1)$ block-Toeplitz matrix defined by toeplitz$(\mathbf{A}_{N\times M}, L) \triangleq [\mathbf{A}_0^T \cdots \mathbf{A}_{L-1}^T]^T$ where $\mathbf{A}_l \triangleq [\mathbf{0}_{N\times l}\ \mathbf{A}_{N\times M}\ \mathbf{0}_{N\times(L-1-l)}]$, and vec$(\mathbf{A})$ forms a vector by stacking columns of $\mathbf{A}$.

2. System Model

This study considers a relaying system with a FF relay node with energy harvesting as shown in Fig. 1. A pair of source ($\mathcal{S}$) and destination ($\mathcal{D}$) nodes communicate via the relay node ($\mathcal{R}$), where a direct path between $\mathcal{S}$ and $\mathcal{D}$ does not exist because of severe pathloss and shadowing. It is assumed that all the channels are frequency-selective, and the received signal suffers from ISI. Both $\mathcal{S}$ and $\mathcal{D}$ operate in half-duplex mode and have a single antenna. Figure 2 shows the structure of the FF relay node, $\mathcal{R}$, equipped with N_t transmit antennas and N_r receive antennas. $\mathcal{R}$ harvests energy from its received signals using the power splitting protocol and has FIR filters that suppress ISI occurring in the whole channel between $\mathcal{S}$ and $\mathcal{D}$.

Figure 3 shows the protocol of the proposed scheme. A time slot with duration T is divided into two phases of $T/2$ each. In the first phase, $\mathcal{S}$ transmits the information symbols with power P_s, while $\mathcal{R}$ harvests energy from a portion of the received signals and processes the remaining portion as information-bearing signals. In the second phase of the remaining $T/2$, the relay node, $\mathcal{R}$, operating in the full-duplex mode transmits the filter outputs toward $\mathcal{D}$, while receiving its own transmitted signals simultaneously[†].

First, the information processing aspect of the proposed scheme is considered. In the first phase, the discrete-time complex envelope of the received signals of $\mathcal{R}$ is represented by a $N_r \times 1$ vector $\mathbf{r}_1[n] = [r_{1,1}[n]\ \cdots r_{1,N_r}[n]]^T$ as

$$\mathbf{r}_1[n] = \frac{1}{\sqrt{d_{\text{SR}}^m}} \sum_{l=0}^{L_f-1} \mathbf{f}_l s[n-l] + \mathbf{m}_1^R[n], \tag{1}$$

where d_{SR} is the distance between $\mathcal{S}$ and $\mathcal{R}$, m is the path loss exponent, $\mathbf{f}_l = [f_{1,l}\ \cdots\ f_{N_r,l}]^T$ is the lth tap of the channels between the relay antennas and $\mathcal{S}$, L_f is the length of the $\mathcal{S}$-to-$\mathcal{R}$ channel impulse responses (CIR), the transmitted symbols $s[n]$ are i.i.d., and $\mathbf{m}_1^R[n]$ is the noise introduced by the receive antenna of $\mathcal{R}$. The received signals are split in $\lambda : 1-\lambda$ proportion for EH and information processing, where λ is the power splitting ratio, $0 < \lambda \leq 1$. The split

[†]As with the previous researches in [7]–[10], although $\mathcal{R}$ operates in the full-duplex mode in the second phase, the proposed system is not a full-duplex system in terms of data transmission. The data transmission rate is the same as the half-duplex system since information reception and forwarding at $\mathcal{R}$ are performed in different phases.

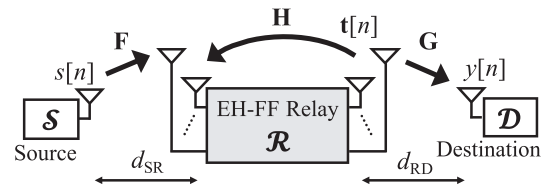

Fig. 1 Relaying system using FF relay with energy harvesting.

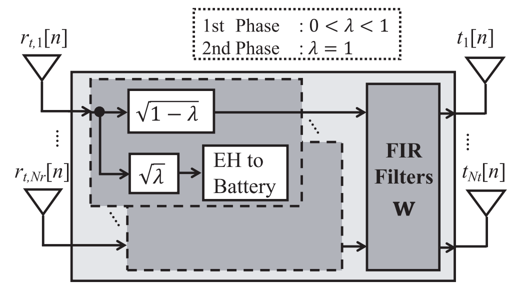

Fig. 2 Structure of FF relay node $\mathcal{R}$ with energy harvesting.

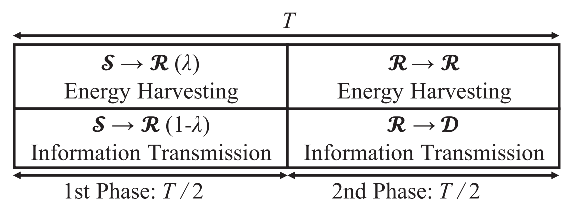

Fig. 3 Protocol of FF relaying with energy harvesting.

signal $\sqrt{1-\lambda}\mathbf{r}_1[n]$ is processed by FIR filters. The baseband output signal of the ith FIR filter at $\mathcal{R}$ is given by

$$t_i[n] = \sum_{l=0}^{L_w-1} \mathbf{w}_{i,l}^H \left(\sqrt{1-\lambda}\mathbf{r}_1[n-l] + \mathbf{z}^R[n-l]\right), \tag{2}$$

where $\mathbf{w}_{i,l} = [w_{1,i,l}\ \cdots\ w_{N_r,i,l}]^T$ is the lth tap coefficient of the ith filter, L_w is the length of the filter impulse response, and $\mathbf{z}^R[n]$ is the noise introduced by RF band to baseband signal conversion at $\mathcal{R}$ [5]. Substituting (1) into (2), we have

$$t_i[n] = \mathbf{w}_i^H \left(\sqrt{\frac{1-\lambda}{d_{\text{SR}}^m}}\bar{\mathbf{F}}\bar{\mathbf{s}}[n] + \sqrt{1-\lambda}\bar{\mathbf{m}}_1^R[n] + \bar{\mathbf{z}}^R[n]\right), \tag{3}$$

where

$$\begin{aligned}
\mathbf{w}_i &\triangleq [\mathbf{w}_{i,0}^T\ \mathbf{w}_{i,1}^T\ \cdots\ \mathbf{w}_{i,L_w-1}^T]^T \in \mathbb{C}^{N_r L_w \times 1},\\
\bar{\mathbf{F}} &\triangleq \text{toeplitz}(\mathbf{F}, L_w) \in \mathbb{C}^{N_r L_w \times (L_f + L_w - 1)},\\
\mathbf{F} &\triangleq [\mathbf{f}_0 \cdots \mathbf{f}_{L_f-1}] \in \mathbb{C}^{N_r \times L_f},\\
\bar{\mathbf{s}}[n] &\triangleq [s[n]\ \cdots\ s[n - L_f - L_w + 2]]^T,\\
\bar{\mathbf{m}}_1^R[n] &\triangleq [(\mathbf{m}_1^R[n])^T\ \cdots\ (\mathbf{m}_1^R[n - L_w + 1])^T]^T,\\
\bar{\mathbf{z}}^R[n] &\triangleq [(\mathbf{z}^R[n])^T\ \cdots\ (\mathbf{z}^R[n - L_w + 1])^T]^T.
\end{aligned}$$

In the second phase, $\mathcal{R}$ transmits the filter outputs $\mathbf{t}[n] = [t_1[n] \cdots t_{N_t}[n]]^T$, while receiving its own transmitted signals passed through loop channels. The complex envelope of the received signal at the ith receive antenna of $\mathcal{R}$ is given by

$$r_{2,i}[n] = \sum_{l=0}^{L_h-1} \mathbf{h}_{i,l}^T \mathbf{t}[n-l] + m_{2,i}^R[n], \quad (4)$$

where $\mathbf{h}_{i,l} = \sqrt{\beta}[h_{1,i,l} \cdots h_{N_t,i,l}]^T$ is the lth tap of the loop channels from the transmit antennas to the ith receive antenna of $\mathcal{R}$, β is the loop channel gain, L_h is the length of the loop CIR, $m_{2,i}^R[n]$ is the noise at the ith receive antenna of $\mathcal{R}$. Note that the received signal from its own transmitter corresponding to the first term in (4) is not harmful since it is not the self-interference, but is rather a useful component as an EH source. The transmitted signals $\mathbf{t}[n]$ pass through channels and are finally received at $\mathcal{D}$. The received signal at $\mathcal{D}$ is given by

$$y[n] = \frac{1}{\sqrt{d_{\mathrm{RD}}^m}} \sum_{i=1}^{N_t-1} \sum_{l=0}^{L_g-1} g_{i,l} t_i[n-l] + v^D[n], \quad (5)$$

where d_{RD} is the distance between $\mathcal{R}$ and $\mathcal{D}$, $g_{i,l}$ is the lth tap of the channel between the ith transmit antenna of $\mathcal{R}$ and $\mathcal{D}$, L_g is the length of the $\mathcal{R}$-to-$\mathcal{D}$ CIR, and $v^D[n]$ is the sum of the antenna and conversion noises at $\mathcal{D}$. Substituting (3) into (5), and after some manipulation, we get

$$\begin{aligned} y[n] &= \mathbf{g}^T \check{\mathbf{W}}^H \left(a\check{\mathbf{F}}\check{\mathbf{s}}[n] + b\check{\mathbf{I}}\check{\mathbf{m}}_1^R[n] + c\check{\mathbf{I}}\check{\mathbf{z}}^R[n]\right) + v^D[n] \quad (6)\\ &= \mathbf{w}^H \check{\mathbf{G}} \left(a\check{\mathbf{F}}\check{\mathbf{s}}[n] + b\check{\mathbf{I}}\check{\mathbf{m}}_1^R[n] + c\check{\mathbf{I}}\check{\mathbf{z}}^R[n]\right) + v^D[n], \quad (7) \end{aligned}$$

where

$$\begin{aligned} & a \triangleq \sqrt{\frac{1-\lambda}{d_{\mathrm{SR}}^m d_{\mathrm{RD}}^m}}, b \triangleq \sqrt{\frac{1-\lambda}{d_{\mathrm{RD}}^m}}, c \triangleq \frac{1}{\sqrt{d_{\mathrm{RD}}^m}},\\ & \check{\mathbf{W}} \triangleq [\mathbf{I}_{L_g} \otimes \mathbf{w}_1^T \cdots \mathbf{I}_{L_g} \otimes \mathbf{w}_{N_t}^T] \in \mathbb{C}^{N_t N_r L_w \times M_t L_g},\\ & \mathbf{w} \triangleq [\mathbf{w}_1^T \cdots \mathbf{w}_{N_t}^T]^T \in \mathbb{C}^{N_t N_r L_w \times 1},\\ & \check{\mathbf{s}}[n] \triangleq \left[s[n]\ s[n-1]\ \cdots\ s[n-L_f-L_w-L_g+3]\right]^T,\\ & \check{\mathbf{m}}_1^R[n] \triangleq \left[(\mathbf{m}_1^R[n])^T \cdots (\mathbf{m}_1^R[n-L_w-L_g+2])^T\right]^T,\\ & \check{\mathbf{z}}^R[n] \triangleq \left[(\mathbf{z}^R[n])^T\ \cdots\ (\mathbf{z}^R[n-L_w-L_g+2])^T\right]^T,\\ & \mathbf{g} \triangleq \mathrm{vec}(\mathbf{G}),\\ & \mathbf{G} \triangleq [\mathbf{g}_1 \cdots \mathbf{g}_{N_t}],\\ & \mathbf{g}_i \triangleq [g_{i,0} \cdots g_{i,L_g-1}]^T,\\ & \check{\mathbf{G}} \triangleq \mathbf{G} \otimes \mathbf{I}_{N_r L_w} \in \mathbb{C}^{N_t N_r L_w \times N_r L_w L_g},\\ & \check{\mathbf{I}} \triangleq [\check{\mathbf{I}}_0^T\ \cdots\ \check{\mathbf{I}}_{L_g-1}^T]^T \in \mathbb{C}^{N_r L_w L_g \times N_r (L_w+L_g-1)},\\ & \check{\mathbf{I}}_l \triangleq [\mathbf{0}_{N_r L_w \times l}\ \mathbf{I}_{N_r L_w}\ \mathbf{0}_{N_r L_w \times (L_g-1-l)}],\\ & \check{\mathbf{F}} \triangleq \mathrm{toeplitz}(\bar{\mathbf{F}}, L_g) \in \mathbb{C}^{N_r L_w L_g \times (L_f+L_w+L_g-2)}. \end{aligned}$$

In (7), the first term $a\mathbf{w}^H\check{\mathbf{G}}\check{\mathbf{F}}\check{\mathbf{s}}[n]$ contains the desired symbol and ISI components. Let the dth entry of $\check{\mathbf{s}}[n]$ be the desired symbol, where d is an arbitrary decision delay. The remaining entries in $\check{\mathbf{s}}[n]$ correspond to the ISI component. Then, we can rewrite (7) as

$$\begin{aligned} y[n] = &\underbrace{a\mathbf{w}^H\check{\mathbf{G}}\tilde{\mathbf{f}}s[n-d+1]}_{y_s[n]:\text{Desired symbol}} + \underbrace{a\mathbf{w}^H\check{\mathbf{G}}\tilde{\mathbf{F}}\tilde{\mathbf{s}}[n]}_{y_i[n]:\text{ISI}}\\ &+ \underbrace{b\mathbf{w}^H\check{\mathbf{G}}\check{\mathbf{I}}\check{\mathbf{m}}^R[n] + c\mathbf{w}^H\check{\mathbf{G}}\check{\mathbf{I}}\check{\mathbf{z}}^R[n] + v^D[n]}_{y_n[n]:\text{Noise}}, \quad (8) \end{aligned}$$

where $\tilde{\mathbf{f}}$ is the dth column of $\check{\mathbf{F}}$, $\tilde{\mathbf{F}}$ is a matrix obtained by removing $\tilde{\mathbf{f}}$ from $\check{\mathbf{F}}$, and $\tilde{\mathbf{s}}[n]$ is a vector obtained by removing $s[n-d+1]$ from $\check{\mathbf{s}}[n]$. In (8), $y_s[n]$, $y_i[n]$ and $y_n[n]$ denote the desired symbol, ISI, and noise components, respectively.

Next, EH operation aspect performed at the relay node $\mathcal{R}$ with N_r receive antennas is considered. In the first phase, $\mathcal{R}$ receives the signals $\mathbf{r}_1[n]$ in (1) from $\mathcal{S}$ and harvests the energy from its power-split signals $\sqrt{\lambda}\mathbf{r}_1[n]$. As the harvested power that originates from the noise is very small, it can be ignored. The harvested power in the first phase can be expressed as [4], [11]

$$p_1 = \eta \mathrm{E}\left[\|\sqrt{\lambda}\mathbf{r}_1[n]\|^2\right] = \eta\lambda\left(\frac{P_s}{d_{\mathrm{SR}}^m}\sum_{i=1}^{N_r}\sum_{l=0}^{L_f-1}|f_{i,l}|^2\right), \quad (9)$$

where $0 < \eta \leq 1$ is the power conversion efficiency, and $P_s \triangleq \mathrm{E}[|s[n]|^2]$. In the second phase, $\mathcal{R}$ harvests energy from $r_{2,i}[n]$ in (4). The harvested power in the second phase is given by

$$p_2 = \eta \sum_{i=1}^{N_r} \mathrm{E}\left[|r_{2,i}[n]|^2\right] = \eta \mathbf{w}^H \mathbf{D}_h \mathbf{w}, \quad (10)$$

where

$$\begin{aligned} & \mathbf{D}_h \triangleq \sum_{i=1}^{N_r} \mathbf{H}_i \tilde{\mathbf{D}} \mathbf{H}_i^H \in \mathbb{C}^{N_t N_r L_w \times N_t N_r L_w},\\ & \mathbf{H}_i \triangleq \left[\mathrm{diag}\{\mathbf{h}_{i,0}^T\} \otimes \mathbf{I}_{N_r L_w} \cdots \mathrm{diag}\{\mathbf{h}_{i,L_h-1}^T\} \otimes \mathbf{I}_{N_r L_w}\right],\\ & \tilde{\mathbf{D}} \triangleq \mathbf{I}_{L_h} \otimes \hat{\mathbf{D}} \in \mathbb{C}^{N_t N_r L_w L_h \times N_t N_r L_w L_h},\\ & \hat{\mathbf{D}} \triangleq \begin{bmatrix} \mathbf{D} & \cdots & \mathbf{D}\\ \vdots & \ddots & \vdots\\ \mathbf{D} & \cdots & \mathbf{D} \end{bmatrix} \in \mathbb{C}^{N_t N_r L_w \times N_t N_r L_w},\\ & \mathbf{D} \triangleq P_s \frac{(1-\lambda)}{d_{\mathrm{SR}}^m} \bar{\mathbf{F}}\bar{\mathbf{F}}^H + (1-\lambda)\sigma_{m_1^R}^2 \mathbf{I}_{N_r L_w} + \sigma_{z^R}^2 \mathbf{I}_{N_r L_w}. \end{aligned}$$

Finally, the total power p_{EH} obtained by the EH processing during two phases is obtained as the sum of (9) and (10), i.e., $p_{EH} = p_1 + p_2$. The relay node, $\mathcal{R}$, uses only the harvested power, p_{EH}, for information transmission. The purpose of the filter design is to determine the FIR filters $\mathbf{w}$ at $\mathcal{R}$, such that the effect of ISI is suppressed and the desired component is enhanced when the relay transmit power is limited to p_{EH}.

3. Filter Design Method

A filter design method for the case where the perfect knowledge of the $\mathcal{R}$-to-$\mathcal{D}$ channels $\{g_{i,l}\}$ is available is considered, and it is shown that the method is also applicable to the case with only partial knowledge of $\{g_{i,l}\}$. Furthermore, the optimum power splitting ratio λ is determined based on the golden-section search.

We assume that $\mathcal{R}$ has the perfect CSI of $\mathcal{S}$-to-$\mathcal{R}$ channels by estimating the channels at $\mathcal{R}$. This assumption is reasonable when the $\mathcal{S}$-to-$\mathcal{R}$ channels remain unchanged for several time slots. We also assume that $\mathcal{R}$ obtains the CSI of $\mathcal{R}$-to-$\mathcal{D}$ channels by feeding back the CSI obtained by channel estimation at $\mathcal{D}$ to $\mathcal{R}$. The feedback uses a low-rate link which does not affect data communication.

3.1 Filter Design Based on Perfect CSI

This case assumes that perfect instantaneous CSI of $\mathcal{R}$-to-$\mathcal{D}$ channels is available at $\mathcal{R}$. This assumption is met if the $\mathcal{R}$-to-$\mathcal{D}$ channels remain unchanged for several time slots. Here, we propose to determine $\mathbf{w}$ so as to maximize the received SINR at $\mathcal{D}$ under a constraint on the relay transmission power. The optimization problem can be formulated as

$$\max_{\mathbf{w}} \ \mathrm{SINR} \quad \text{s.t.} \ p_t \le p_{EH}, \tag{11}$$

where p_t is the power consumed at $\mathcal{R}$ for signal transmission, which is expressed as

$$p_t = \sum_{i=1}^{N_t} \mathrm{E}[|t_i[n]|^2] = \mathbf{w}^H \bar{\mathbf{D}} \mathbf{w}, \tag{12}$$

where

$$\bar{\mathbf{D}} \triangleq \mathbf{I}_{N_t} \otimes \mathbf{D} \in \mathbb{C}^{N_t N_r L_w \times N_t N_r L_w}.$$

The constraint ensures that the transmitted power of the relay node does not exceed the harvested power p_{EH}. From (8), we have the received SINR at $\mathcal{D}$ as

$$\mathrm{SINR} = \frac{\mathbf{w}^H \mathbf{Q}_s \mathbf{w}}{\mathbf{w}^H \mathbf{Q}_i \mathbf{w} + \mathbf{w}^H \mathbf{Q}_n \mathbf{w} + \sigma^2_{v^D}}, \tag{13}$$

where

$$\mathbf{Q}_s \triangleq a^2 P_s \check{\mathbf{G}} \tilde{\mathbf{f}} \tilde{\mathbf{f}}^H \check{\mathbf{G}}^H,$$
$$\mathbf{Q}_i \triangleq a^2 P_s \check{\mathbf{G}} \tilde{\mathbf{F}} \tilde{\mathbf{F}}^H \check{\mathbf{G}}^H,$$
$$\mathbf{Q}_n \triangleq \left(b^2 \sigma^2_{m_1^R} + c^2 \sigma^2_{z^R}\right) \check{\mathbf{G}} \check{\mathbf{I}} \check{\mathbf{I}}^H \check{\mathbf{G}}^H,$$

and $\sigma^2_{v^D}, \sigma^2_{m_1^R}, \sigma^2_{z^R}$ are the power of $v^D[n], m^R_{1,i}[n], z^R_i[n]$, respectively. Using (9), (10), (12), (13), we can write (11) as

$$\max_{\mathbf{w}} \ \frac{\mathbf{w}^H \mathbf{Q}_s \mathbf{w}}{\mathbf{w}^H \mathbf{Q}_{i+n} \mathbf{w} + \sigma^2_{v^D}} \qquad \text{s.t.} \ \mathbf{w}^H \check{\mathbf{D}} \mathbf{w} \le p_1, \tag{14}$$

where $\mathbf{Q}_{i+n} \triangleq \mathbf{Q}_i + \mathbf{Q}_n$ and $\check{\mathbf{D}} \triangleq \bar{\mathbf{D}} - \eta \mathbf{D}_h$. By introducing a vector $\tilde{\mathbf{w}} \triangleq \check{\mathbf{D}}^{1/2} \mathbf{w}$, we can rewrite (14) as

$$\max_{\mathbf{w}} \ \frac{\tilde{\mathbf{w}}^H \tilde{\mathbf{Q}}_s \tilde{\mathbf{w}}}{\tilde{\mathbf{w}}^H \tilde{\mathbf{Q}}_{i+n} \tilde{\mathbf{w}} + \sigma^2_{v^D}} \qquad \text{s.t.} \ \|\tilde{\mathbf{w}}\|^2 \le p_1, \tag{15}$$

where $\tilde{\mathbf{Q}}_s \triangleq \check{\mathbf{D}}^{-1/2} \mathbf{Q}_s \check{\mathbf{D}}^{-1/2}$ and $\tilde{\mathbf{Q}}_{i+n} \triangleq \check{\mathbf{D}}^{-1/2} \mathbf{Q}_{i+n} \check{\mathbf{D}}^{-1/2}$. The objective function in (15) monotonically increases as $\|\tilde{\mathbf{w}}\|^2$ increases since it can be expressed as $\hat{\mathbf{w}}^H \tilde{\mathbf{Q}}_s \hat{\mathbf{w}} / (\hat{\mathbf{w}}^H \tilde{\mathbf{Q}}_{i+n} \hat{\mathbf{w}} + \sigma^2_{v^D} / \|\tilde{\mathbf{w}}\|^2)$ where $\hat{\mathbf{w}} = \tilde{\mathbf{w}} / \|\tilde{\mathbf{w}}\|$. The objective function is maximized when $\|\tilde{\mathbf{w}}\|^2 = p_1$, and hence the constraint in (15) becomes $\|\tilde{\mathbf{w}}\|^2 = p_1$. As a result, the optimization problem (15) can be treated as a generalized eigenvalue problem [6], [14] and the solution is obtained by the following equation.

$$\tilde{\mathbf{w}}_{\mathrm{opt}} = \sqrt{p_1} \mathcal{P} \left\{ \tilde{\mathbf{Q}}_s, \tilde{\mathbf{Q}}_{i+n} + (\sigma^2_{v^D}/p_1) \mathbf{I}_{N_r N_t L_w} \right\}, \tag{16}$$

where $\mathcal{P}\{\mathbf{A}, \mathbf{B}\}$ denotes the normalized principal generalized eigenvector of the matrix pair $(\mathbf{A}, \mathbf{B})$. Finally, the optimal filter coefficients $\mathbf{w}_{\mathrm{opt}}$ are obtained, and the maximum SINR at $\mathcal{D}$ can be written as

$$\mathbf{w}_{\mathrm{opt}} = \check{\mathbf{D}}^{-1/2} \tilde{\mathbf{w}}_{\mathrm{opt}}, \tag{17}$$

$$\mathrm{SINR}_{\max} = \mathcal{L}_{\max} \left\{ \tilde{\mathbf{Q}}_s, \tilde{\mathbf{Q}}_{i+n} + (\sigma^2_{v^D}/p_1) \mathbf{I}_{N_r N_t L_w} \right\}, \tag{18}$$

where $\mathcal{L}_{\max}\{\mathbf{A}, \mathbf{B}\}$ denotes the largest generalized eigenvalue of matrix pair $(\mathbf{A}, \mathbf{B})$. Note that the computational complexity of the proposed method is governed by the generalized eigenvalue decomposition in (16), whose complexity is $O\left((N_t N_r L_w)^3\right)$ [13].

3.2 Filter Design Based on Partial CSI

In the previous subsection, it was assumed that $\mathcal{R}$ has the perfect knowledge of the CSI of $\mathcal{R}$-to-$\mathcal{D}$ channels. However, this assumption might not be reasonable in some cases such as the $\mathcal{R}$-to-$\mathcal{D}$ channels change rapidly, and thus channel estimation and CSI feedback consume communication resources. Here, we consider the case where only the second-order statistics (SOS), which are less burdensome than the perfect CSI, of $\mathcal{R}$-to-$\mathcal{D}$ channels are available at $\mathcal{R}$.

First, the power of the desired signal component in (8) can be rewritten as[†]

$$\begin{aligned}
\mathrm{E}\left[|y_s[n]|^2\right] &= a^2 P_s \mathrm{trace}(\tilde{\mathbf{f}}^H \check{\mathbf{W}} \mathrm{E}[\mathbf{g}^* \mathbf{g}^T] \check{\mathbf{W}}^H \tilde{\mathbf{f}}) \\
&= a^2 P_s \mathrm{trace}(\check{\mathbf{W}}^H \tilde{\mathbf{f}} \tilde{\mathbf{f}}^H \check{\mathbf{W}} \mathbf{R}_g^*) \\
&= a^2 P_s \mathrm{vec}(\check{\mathbf{W}}^*)^T (\mathbf{R}_g^H \otimes \tilde{\mathbf{f}} \tilde{\mathbf{f}}^H) \mathrm{vec}(\check{\mathbf{W}}) \\
&= a^2 P_s \mathbf{w}^H \mathbf{M}^H (\mathbf{R}_g^H \otimes \tilde{\mathbf{f}} \tilde{\mathbf{f}}^H) \mathbf{M} \mathbf{w} \\
&\triangleq \mathbf{w}^H \mathbf{Q}_s^{\mathrm{sos}} \mathbf{w},
\end{aligned} \tag{19}$$

where $\mathbf{R}_g = \mathrm{E}[\mathbf{g}\mathbf{g}^H]$ represents the SOS of $\mathcal{R}$-$\mathcal{D}$ channels,

$$\mathbf{M} \triangleq [\mathbf{M}_{1,1} \cdots \mathbf{M}_{1,L_g} \cdots \mathbf{M}_{N_t,1} \cdots \mathbf{M}_{N_t,L_g}]^T,$$
$$\mathbf{M}_{i,l} \triangleq [\mathbf{0}_{N_t N_r L_w \times ((l-1) N_r L_w)} \ \tilde{\mathbf{M}}_i^T \ \mathbf{0}_{N_t N_r L_w \times ((L_g - l) N_r L_w)}],$$
$$\tilde{\mathbf{M}}_i \triangleq [\mathbf{0}_{N_r L_w \times (i-1) N_r L_w} \ \mathbf{I}_{N_r L_w} \ \mathbf{0}_{N_r L_w \times (N_t - i) N_r L_w}].$$

In the same way, the power of ISI and noise components can

[†]We use $\mathrm{trace}(\mathbf{ABCD}) = [\mathrm{vec}(\mathbf{A}^T)]^T (\mathbf{D}^T \otimes \mathbf{B}) \mathrm{vec}(\mathbf{C})$ to derive the third line from the second line.

be rewritten. Then we obtain the received SINR at $\mathcal{D}$ as

$$\mathrm{SINR}^{\mathrm{sos}} = \frac{\mathbf{w}^H \mathbf{Q}_s^{\mathrm{sos}} \mathbf{w}}{\mathbf{w}^H \mathbf{Q}_{i+n}^{\mathrm{sos}} \mathbf{w} + \sigma_{vD}^2}, \tag{20}$$

where $\mathbf{Q}_{i+n}^{\mathrm{sos}} \triangleq \mathbf{Q}_i^{\mathrm{sos}} + \mathbf{Q}_n^{\mathrm{sos}}$,

$$\mathbf{Q}_i^{\mathrm{sos}} \triangleq a^2 P_s \mathbf{M}^H (\mathbf{R}_g^H \otimes \tilde{\mathbf{F}}\tilde{\mathbf{F}}^H)\mathbf{M}, \tag{21}$$

$$\mathbf{Q}_n^{\mathrm{sos}} \triangleq \left(b^2 \sigma_{m_1^R}^2 + c^2 \sigma_{z^R}^2\right) \mathbf{M}^H (\mathbf{R}_g^H \otimes \breve{\mathbf{I}}\breve{\mathbf{I}}^H)\mathbf{M}. \tag{22}$$

The SINR in (20) is the same form as that in (14). In a similar way as shown in Sect. 3.1, the optimal filter coefficients $\mathbf{w}_{\mathrm{opt}}^{\mathrm{sos}}$ can be obtained, which maximize the SINR (20) under the relay transmit power constraint as

$$\mathbf{w}_{\mathrm{opt}}^{\mathrm{sos}} = \breve{\mathbf{D}}^{-1/2} \tilde{\mathbf{w}}_{\mathrm{opt}}^{\mathrm{sos}}, \tag{23}$$

$$\tilde{\mathbf{w}}_{\mathrm{opt}}^{\mathrm{sos}} = \sqrt{p_1} \mathcal{P} \left\{ \tilde{\mathbf{Q}}_s^{\mathrm{sos}}, \tilde{\mathbf{Q}}_{i+n}^{\mathrm{sos}} + (\sigma_{vD}^2 / p_1) \mathbf{I}_{N_r N_t L_w} \right\}, \tag{24}$$

where $\tilde{\mathbf{Q}}_s^{\mathrm{sos}} \triangleq \breve{\mathbf{D}}^{-1/2} \mathbf{Q}_s^{\mathrm{sos}} \breve{\mathbf{D}}^{-1/2}$ and $\tilde{\mathbf{Q}}_{i+n}^{\mathrm{sos}} \triangleq \breve{\mathbf{D}}^{-1/2} \mathbf{Q}_{i+n}^{\mathrm{sos}} \breve{\mathbf{D}}^{-1/2}$. Also, the SINR is obtained as

$$\mathrm{SINR}_{\max}^{\mathrm{sos}} = \mathcal{L}_{\max} \left\{ \tilde{\mathbf{Q}}_s^{\mathrm{sos}}, \tilde{\mathbf{Q}}_{i+n}^{\mathrm{sos}} + (\sigma_{vD}^2 / p_1) \mathbf{I}_{N_r N_t L_w} \right\}. \tag{25}$$

3.3 Determination of Power Splitting Ratio

In the filter design method explained above, the power-splitting ratio λ is given. As will be shown in the next section, λ affects the received SINR at $\mathcal{D}$. Therefore, it is important to appropriately determine λ. If λ is too small, the amount of the harvested energy becomes low, while if λ is too large, the magnitude of the information-conveying signal becomes small. Since the SINR degrades in both cases, it might be assumed that the SINR is a unimodal function of λ. As the golden-section search (GSS) method is efficient in finding the extremum of a unimodal function [15], it is employed to find the maximum value of the SINR. In **Algorithm**, the optimum value of λ is searched by iteratively updating tentative SINR and λ without calculating the filter coefficients at each iteration. The determination process of λ by the GSS method is summarized in **Algorithm**. After λ_{opt} is determined, the optimal filter coefficients $\mathbf{w}_{\mathrm{opt}}$ are computed using (17) or (23).

4. Simulation Results

Simulation results have been provided for the performance evaluation of the proposed scheme. Unless otherwise stated, the simulation parameters are as follows: the number of transmit and receive antennas are $N_t = 2$ and $N_r = 2$, the length of the FIR filters is $L_w = 3$, the power conversion efficiency is $\eta = 0.5$, the source transmission power $P_s = 20\,\mathrm{dBm}$, the power of all noises is $-70\,\mathrm{dBm}$, the modulation scheme is quadrature phase shift keying (QPSK), the termination tolerance of the golden-section search is $\epsilon_\lambda = 10^{-2}$, the distance between $\mathcal{S}$ and $\mathcal{R}$ is $d_{\mathrm{SR}} = 20$, the distance between $\mathcal{R}$ and $\mathcal{D}$ is $d_{\mathrm{RD}} = 15$, the path loss exponent is $m = 3$, the loop channel gain is $\beta = -15\,\mathrm{dB}$, the CIRs $\mathbf{f}_l, \mathbf{g}_l, \mathbf{h}_l$ are modeled as zero-mean, unit-variance, complex Gaussian random variables, and their lengths are $L_f = L_g = 3$ and $L_h = 2$, respectively. Average SINR and bit error rate (BER) are obtained from 10^3 simulation trials, where each trail has independent channel realization and 10^6 data symbols.

Algorithm Determination of the power splitting ratio λ

Initialization: Set $[A, B] = [0, 1]$, $\phi = \frac{1+\sqrt{5}}{2}$, $\lambda_l^{(1)} = (A\phi + B)/2$, $\lambda_u^{(1)} = (A + B\phi)/2$, $n = 1$.
Compute $\mathrm{SINR}_{\lambda_l}^{(1)}$ for $\lambda_l^{(1)}$ and $\mathrm{SINR}_{\lambda_u}^{(1)}$ for $\lambda_u^{(1)}$ using (18) or (25).
while $|\mathrm{SINR}_{\lambda_l}^{(n)} - \mathrm{SINR}_{\lambda_u}^{(n)}| \geq \epsilon_\lambda$ **do**
  if $\mathrm{SINR}_{\lambda_l}^{(n)} < \mathrm{SINR}_{\lambda_u}^{(n)}$ **then**
    Set $A \leftarrow \lambda_l^{(n)}$ and $\mathrm{SINR}_{\lambda_l}^{(n+1)} \leftarrow \mathrm{SINR}_{\lambda_u}^{(n)}$.
    Set $\lambda_u^{(n+1)} = (A + B\phi)/2$.
    Compute $\mathrm{SINR}_{\lambda_u}^{(n+1)}$ for $\lambda_u^{(n+1)}$ using (18) or (25).
  else $\{\mathrm{SINR}_{\lambda_l}^{(n)} > \mathrm{SINR}_{\lambda_u}^{(n)}\}$
    Set $B \leftarrow \lambda_u^{(n)}$ and $\mathrm{SINR}_{\lambda_u}^{(n+1)} \leftarrow \mathrm{SINR}_{\lambda_l}^{(n)}$.
    Set $\lambda_l^{(n+1)} = (A\phi + B)/2$.
    Compute $\mathrm{SINR}_{\lambda_l}^{(n+1)}$ for $\lambda_l^{(n+1)}$ using (18) or (25).
  end if
  Set $n = n + 1$
end while
if $\mathrm{SINR}_{\lambda_l}^{(n+1)} > \mathrm{SINR}_{\lambda_u}^{(n+1)}$ **then** $\lambda_{\mathrm{opt}} = \lambda_l$ **else** $\lambda_{\mathrm{opt}} = \lambda_u$.

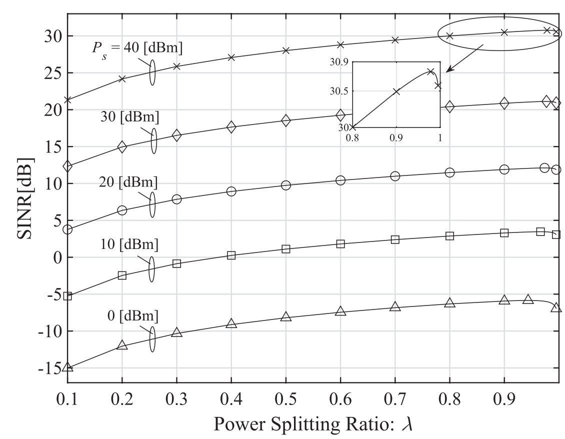

Fig. 4 Relation between SINR and power splitting ratio λ.

The GSS method used in **Algorithm** can be applied to unimodal functions. Since it is difficult to theoretically prove the unimodality of the average SINR with respect to the power splitting ratio λ, we confirm it numerically. Figure 4 shows the average SINR at $\mathcal{D}$ as a function of λ. It can be observed that the average SINR is a unimodal function of λ. Therefore, the method described in 3.3 can effectively find the optimum value of λ. It can also be seen that the optimum value of λ is close to 1.0. This implies that most of the received signal should be used as energy source rather than for information processing, in an energy-restricted relay node.

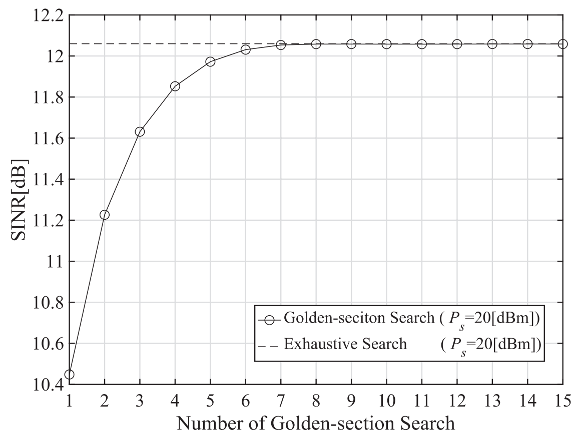

Fig. 5 SINR evolution through power splitting ratio determination algorithm.

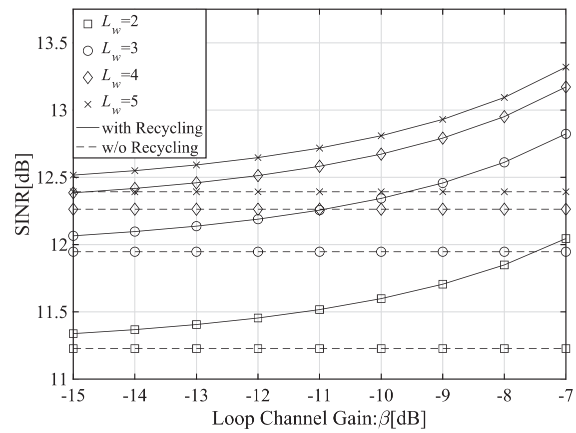

Fig. 7 Effect of loop channel gain β on SINR.

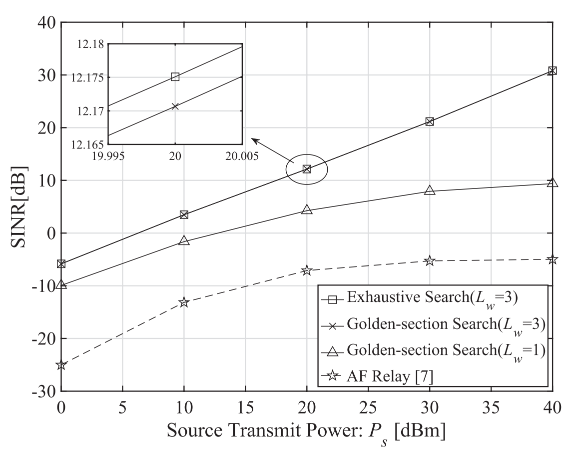

Fig. 6 Effect of source transmission power P_s on SINR.

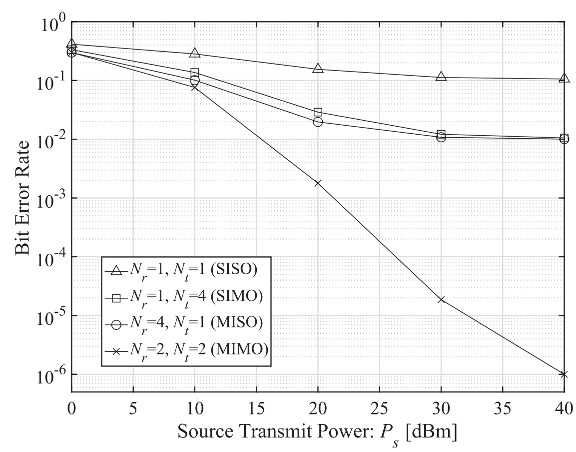

Fig. 8 BER performance for various antenna configurations.

In Fig. 5, the SINR evolution is illustrated using the power splitting ratio determination algorithm. For comparison, the result when the exhaustive search of λ is performed is also shown. As expected, it is seen that the performance of the proposed algorithm improves as the number of iterations increase, and that the performance of the proposed algorithm hardly changes after 8 iterations.

Figure 6 shows the effects on SINR when the source transmission power P_s is varied. It can be observed that the performance of the proposed method with $L_w = 3$ is close to that of the exhaustive search of λ, and that the performance improves as the source transmit power P_s increases. This is because the energy p_{EH} harvested by the relay node increases as P_s increases. For comparison purposes, we also show the results of the AF scheme [7] and the proposed method with $L_w = 1$, where the relay design method in [7] is applied to an AF relay node corresponding to $L_w = 1$ by ignoring the delayed waves in the channels. Note that it is not straightforward to apply the AF scheme [7] to OFDM because the AF relay design cannot be done per subcarrier basis due to the dependency of the harvested energy on all the subcarriers. It is clear that the performance of the AF scheme is poor because it cannot suppress ISI. In addition, we can see that the performance of the AF scheme is worse than that of the proposed method with $L_w = 1$. This is because the AF scheme cannot harvest the energy from the delayed waves efficiently.

The effect of the loop channel gain β at $\mathcal{R}$ is shown in Fig. 7. It can be seen that the performance of the proposed scheme is always better than when there is no self-energy recycling; therefore, confirming its importance. It can also be observed that the performance of the proposed scheme improves with β because the harvested energy p_{EH} increases as β increases.

Figure 8 shows the average BER against the source transmission power, P_s, for various antenna configurations. Four types of relays have been compared, i.e., SISO, SIMO, MISO, and MIMO. The relays other than MIMO experience error floor in BER curves because they cannot suppress ISI significantly. Unlike them, the BER of the MIMO relay decreases as the source transmit power P_s increases, because the MIMO relay has a capability to suppress ISI completely.

The ISI suppression capability can be explained in more detail as follows. The ISI suppression in the system shown in Fig. 1 can be viewed as a multichannel equalization problem where there are $N_r N_t$ subchannels whose CIR is $c_{i,j,l} =$

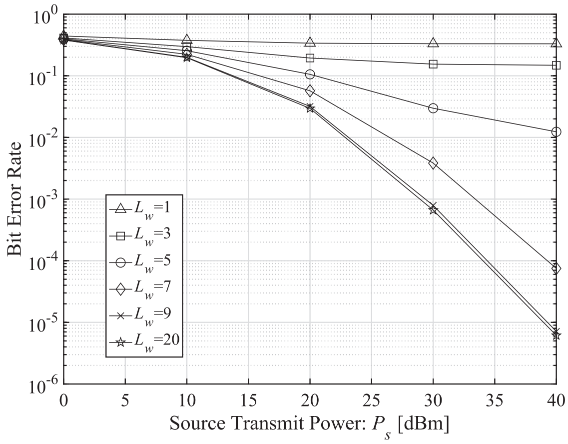

Fig. 9 BER performance for various filter lengths L_w.

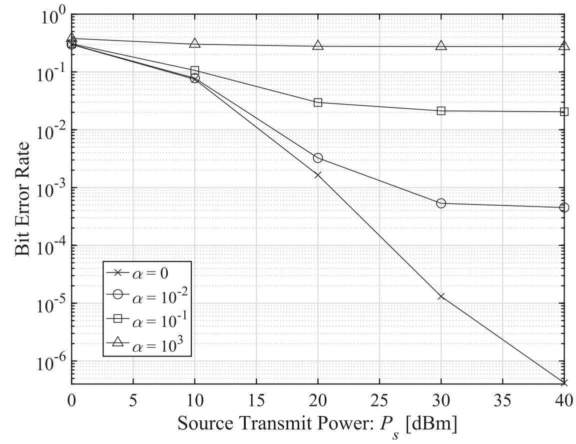

Fig. 10 BER performances for various uncertainty levels α.

$f_{i,l} * g_{j,l}$ and $N_r N_t$ corresponding FIR equalizers $w_{i,j,l}$ for $i = 1, \cdots, N_r, j = 1, \cdots, N_t$. Our primary purpose is to achieve the zero-forcing (ZF) equalization which suppresses ISI completely in the absence of noise; in other words, to find $\mathbf{w}$ such that $\mathbf{w}^H \mathbf{C} = [1\ 0\ \cdots\ 0]$ where $\mathbf{C} = \left[\breve{\mathbf{G}}\tilde{\mathbf{f}}\ \ \breve{\mathbf{G}}\tilde{\mathbf{F}}\right]$ from (8). It is known that the ZF equalization by FIR filters can be achieved if and only if the subchannels $\{c_{i,j,l}\}$ have no common zeros [12]. In the case of SISO, this condition is not met because there is only one subchannel. In the case of SIMO and MISO, the condition is not met because the subchannels contains a common channel, $f_{1,l}$ for SIMO and $g_{1,l}$ for MISO. Thus, only MIMO relay can satisfy the condition. When the ZF equalization can be achieved, the matrix, $\mathbf{C}$, whose size is $N_t N_r L_w \times (L_f + L_w + L_g - 2)$ has full column rank [12], and we have

$$N_t N_r L_w \geq L_f + L_w + L_g - 2. \tag{26}$$

As this condition can also be satisfied by increasing the number of relay antennas N_t or N_r, the MIMO configuration is again preferable. Note that increasing the number of antennas or the filter length results in not only ISI suppression, but also significant performance improvement.

In Fig. 9, BER performances are shown for various filter lengths L_w. It can be seen that the performance of the AF scheme using self-energy recycling, which corresponds to the case with $L_w = 1$, hardly improves even if the source transmission power, P_s, increases. This is because the AF scheme cannot compensate for severe ISI. Meanwhile, the performance of the proposed FF scheme ($L_w > 1$) is effective because of its ISI suppression capability. Also, it can be seen that the performance improves as L_w increases up to $L_w = 9$.

Finally, the case where only the SOS of $\mathcal{R}$-to-$\mathcal{D}$ channels are available is considered. The following model is employed for the $\mathcal{R}$-to-$\mathcal{D}$ CIRs [14]:

$$g_{i,l} \triangleq \frac{1}{\sqrt{1+\alpha}}(\hat{g}_{i,l} + \sqrt{\alpha}\tilde{g}_{i,l}), \tag{27}$$

where $\hat{g}_{i,l}$ and $\tilde{g}_{i,l} \sim \mathcal{CN}(0,1)$ are the mean and variable components of $g_{i,l}$, and α is a parameter which controls the level of uncertainty in $g_{i,l}$. Then, the SOS of $\mathcal{R}$-to-$\mathcal{D}$ channels is given by

$$\mathbf{R}_g = \mathrm{E}[\mathbf{g}\mathbf{g}^H] = \frac{1}{1+\alpha}(\hat{\mathbf{g}}\hat{\mathbf{g}}^H + \alpha \mathbf{I}_{N_t L_g}), \tag{28}$$

where $\hat{\mathbf{g}} \triangleq [\hat{\mathbf{g}}_1^T \cdots \hat{\mathbf{g}}_{N_t}^T]^T$. In each simulation trial, a mean value $\hat{g}_{i,l}$ was generated and 10^2 realizations of $\tilde{g}_{i,l}$ were generated. Figure 10 plots the BER performances for various α. For reference, two extreme cases are shown, $\alpha = 0$ corresponding to the perfect CSI ($\mathbf{R}_g = \mathbf{g}\mathbf{g}^H$) and $\alpha = 10^3$ corresponding to no CSI ($\mathbf{R}_g \approx \mathbf{I}_{N_t L_g}$). It can be seen that the performance of the case with SOS ($\alpha = 10^{-1}$ or 10^{-2}) is significantly better than that of the case with no CSI ($\alpha = 10^3$). This implies that the SOS is useful when the perfect CSI is unavailable.

5. Conclusion

This paper has investigated a filter-and-forward relay with self-energy recycling for single-carrier transmission in frequency-selective channels. In this study, we have proposed the filter design method and the determination algorithm of the power splitting ratio. Simulation results showed that the proposed algorithm can provide the power splitting ratio close to the optimum value. It was also shown that filtering and self-energy recycling are effective in improving performance. Moreover, it was observed that the proposed method works well even when only the partial CSI for relay-destination channels is available.

References

[1] X. Lu, P. Wang, D. Niyato, D.I. Kim, and Z. Han, "Wireless charging technologies: Fundamentals, standards, and network applications," IEEE Commun. Surveys Tuts., vol.18, no.2, pp.1413–1452, 2nd Quart. 2016.

[2] X. Lu, P. Wang, D. Niyato, D.I. Kim, and Z. Han, "Wireless networks with RF energy harvesting: A contemporary survey," IEEE Commun. Surveys Tuts., vol.17, no.2, pp.757–789, 2nd Quart. 2015.

[3] T.D.P. Perera, D.N.K. Jayakody, S.K. Sharma, S. Chatzinotas, and J. Li, "Simultaneous wireless information and power transfer (SWIPT): Recent advances and future challenges," IEEE Commun. Surveys

Tuts., vol.20, no.1, pp.264–302, 2018.
[4] R. Zhang and C.K. Ho, "MIMO broadcasting for simultaneous wireless information and power transfer," IEEE Trans. Wireless Commun., vol.12, no.5, pp.1989–2001, May 2013.
[5] A.A. Nasir, X. Zhou, S. Durrani, and R.A. Kennedy, "Relaying protocols for wireless energy harvesting and information processing," IEEE Trans. Wireless Commun., vol.12, no.7, pp.3622–3636, July 2013.
[6] H. Chen, A.B. Gershman, and S. Shahbazpanahi, "Filter-and-forward distributed beamforming in relay networks with frequency selective fading," IEEE Trans. Signal Process., vol.58, no.3, pp.1251–1262, March 2010.
[7] Y. Zeng and R. Zhang, "Full-duplex wireless-powered relay with self-energy recycling," IEEE Wireless Commun. Lett., vol.4, no.2, pp.201–204, April 2015.
[8] D. Hwang, K.C. Hwang, D.I. Kim, and T.J. Lee, "Self-energy recycling for RF powered multi-antenna relay channels," IEEE Trans Wireless Commun., vol.16, no.2, pp.812–824, Feb. 2017.
[9] Ö.T. Demir and T.E. Tuncer, "Optimum QoS-aware beamformer design for full-duplex relay with self-energy recycling," IEEE Wireless Commun. Lett., vol.7, no.11, pp.122–125, Feb. 2018.
[10] C. Li, W. Wen, P. Wu, and M. Xia, "Wirelessly-powered full-duplex AF MIMO relay systems based on antenna switching," IEEE Commun. Lett., vol.23, no.9, pp.1640–1643, Sept. 2019.
[11] Y. Zeng and R. Zhang, "Optimized training for net energy maximization in multi-antenna wireless energy transfer over frequency-selective channel," IEEE Trans. Commun., vol.63, no.6, pp.2360–2373, June 2015.
[12] E. Bai and Z. Ding, "Zero-forcing equalizability of FIR and IIR multichannel systems with and without perfect measurements," IEEE Trans. Commun., vol.48, pp.17–22, Jan. 2000.
[13] G.H. Golub and C.F. Van Loan, Matrix Computations, 3rd ed., The Johns Hopkins University Press, Baltimore, 1996.
[14] V. Havary-Nassab, S. Shahbazpanahi, A. Grami, and Z.Q. Luo, "Distributed beamforming for relay networks based on second-order statistics of the channel state information," IEEE Trans. Signal Process., vol.56, no.9, pp.4306–4316, Sept. 2008.
[15] W.H. Press, S.A. Teukolsky, W.T. Vetterling, and B.P. Flannery, Numerical Recipes in C, Cambridge University Press, 1992.

Junta Furukawa received B.Eng. and M.Eng. degrees in electrical and electronic engineering from Ibaraki University, Hitachi, Japan, in 2018 and 2020, respectively. In 2020, he joined NTT Electronics Corp., Kanagawa, Japan. His research interests include signal processing for wireless communications.

Teruyuki Miyajima received B.Eng., M.Eng., and Ph.D. degrees in electrical engineering from Saitama University, Saitama, Japan, in 1989, 1991, and 1994, respectively. In 1994, he joined Ibaraki University, Hitachi, Japan, where he is currently a professor in the domain of electrical and electronic systems engineering. His current interests are in signal processing for wireless communications. Dr. Miyajima is a member of IEEE.

Yoshiki Sugitani received M.Eng., and Ph.D. degrees in electrical engineering from Osaka Prefecture University, Sakai, Japan, in 2013 and 2016, respectively. In 2016, he joined Ibaraki University, Hitachi, Japan, where he is currently an assistant professor in the domain of electrical and electronic systems engineering. His current interests are in control for synchronization of complex networks. Dr. Sugitani is a member of IEICE.